Combining Directional Light Output and Ultralow Loss in Deformed Microdisks

Jan Wiersig
Institut für Theoretische Physik, Universität Bremen, Postfach 330 440, D-28334 Bremen, Germany

Martina Hentschel
Max-Planck-Institut für Physik komplexer Systeme, Nöthnitzer Straße 38, D-01187 Dresden, Germany

(Received 27 April 2007; revised manuscript received 23 November 2007; published 23 January 2008)

A drawback of optical modes in microdisk cavities is their isotropic light emission. Here we report a novel, robust, and general mechanism that results in highly directional light emission from high-quality modes. This surprising finding is explained by a combination of wave phenomena (wave localization along unstable periodic ray trajectories) and chaotic ray dynamics in open systems (escape along unstable manifolds) and applies even to microlasers operating in the common multimode regime. We demonstrate our novel mechanism for the limaçon cavity and find directional emission with narrow angular divergence for a significant range of geometries and material parameters.

DOI: 10.1103/PhysRevLett.100.033901 PACS numbers: 42.55.Sa, 05.45.Mt, 42.25.−p, 42.60.Da

The possibility to confine photons in all three spatial dimensions using microcavities has triggered intense basic and applied research in physics over the past decade [1], e.g., research on ultralow threshold lasing [2,3], single-photon emitters [4], and solid-state cavity quantum electrodynamics [5–7]. Prominent examples of optical microcavities are whispering-gallery cavities such as microdisks [8–10], microspheres [11–13], and microtoroids [14–16] which trap photons for a long time τ near the boundary by total internal reflection. The corresponding whispering-gallery modes have very high quality factors $Q = \omega\tau$, where ω is the resonance frequency. The record Q factor is around 7×10^5 for semiconductors [9] and 6×10^7 for silica microdisks [10]. The high Q factors and the in-plane light emission make microdisks attractive candidates for several optoelectronic devices, especially for the nitride material system [17] where other cavity designs such as vertical-cavity surface-emitting laser (VCSEL) micropillars face severe challenges in mirror fabrications [18]. Unfortunately, the possible use of microdisks is limited by the fact that the in-plane light emission is isotropic.

Shortly after the first fabrication of microdisks it was demonstrated that deforming the boundary of a disk allows for improved directionality of emission and therefore for more efficient extraction and collection of light [19–22]. Several shapes have been proposed and realized since then, but only a few lead to light emission into roughly a single direction [23,24] that is essential for applications like single-photon sources. Moreover, all deformed microdisks discussed in the literature have a serious problem, Q spoiling [25]: The Q factor degrades dramatically upon deformation, in the worst case ruling out any application. The trade-off between the Q factor and directionality is not only a problem of microdisks but also of microspheres, microtoroids, and even of VCSEL micropillars [26].

Recently, a scheme to achieve highly directional emission without Q spoiling has been suggested [27]. It employs the characteristic modifications of spatial mode structures near avoided resonance crossings. The drawback of this approach is the existence of nearly degenerate modes which can have different far-field patterns (FFPs). If two such modes are excited simultaneously (typical for present-day devices), the directionality might be lost. Nearly degenerate modes with similar FFP do occur, but to find them requires laborious numerical calculations and a sophisticated adjustment of geometry parameters depending on refractive index, wavelength, and cavity size.

In this Letter we introduce a novel, robust, and generally applicable mechanism to achieve highly directional light emission from high-Q modes in microdisks which does not suffer from the above-mentioned drawback. The key to our finding is to apply what is at the heart of quantum chaos [28] and nonlinear dynamics [29] of open systems, respectively: wave localization along unstable periodic ray trajectories in systems with chaotic ray dynamics [30] and the only recently acknowledged importance of the so-called unstable manifold for the FFPs of microcavities [31–34]. The wave localization ensures the desired high Q factors, whereas the unstable manifold provides the directional emission. Concerning the realization of this scheme in practice, adequate microcavity devices can be expected to be easy to fabricate as no sophisticated adjustment of parameters is required. They are, moreover, well suited for multimode laser operation as all high-Q modes of a given polarization possess similar FFPs.

A microdisk is a quasi-two-dimensional system described by an effective index of refraction n. We assume $n = 3.3$ (GaAs) both for transverse magnetic (TM) and transverse electric (TE) polarization. A slight polarization dependence of n is neglected; it could be adjusted in the fabrication process, e.g., by changing the slab thickness. For the boundary curve of the deformed microdisk we choose the limaçon of Pascal which reads in polar coordinates $\rho(\phi) = R(1 + \varepsilon\cos\phi)$. Ray and wave dynamics in the corresponding family of closed cavities (''limaçon billiards'') have been discussed in the field of quantum

chaos [35]. The limiting case of vanishing deformation parameter ε is the circle with radius R. Figure 1(a) illustrates a whispering-gallery ray trajectory in a circular microdisk trapped by total internal reflection. A two-dimensional phase space representation, the so-called Poincaré surface of section (SOS), is shown in Fig. 1(b). Whenever the trajectory hits the cavity's boundary, its position s (arclength coordinate along the circumference) and tangential momentum $\sin\chi$ (the angle of incidence χ is measured from the surface normal) is recorded. For $\varepsilon = 0$, rotational invariance of the system implies conservation of the angular momentum $\propto \sin\chi$. Ignoring wave effects, such a ray never leaves the cavity since it cannot enter the leaky region between the two critical lines for total internal reflection given by $\sin\chi_c = \pm 1/n$.

Figures 1(c) and 1(d) show a trajectory in the limaçon cavity for $\varepsilon = 0.43$. In contrast to the case of small deformation parameter ε [25] the dynamics is predominantly chaotic. Starting with an initial χ well above the critical line, a test ray (square, thick dots, and triangle) rapidly approaches the leaky region ($\sin\chi$ is not conserved) where it escapes according to Snell's and Fresnel's laws. Without refractive escape ($n = \infty$, hard wall or closed billiard limit), the trajectory would fill the phase space in a random fashion (small dots). Periodic ray trajectories do exist but are always unstable, except for the two islands in the leaky region. Whispering-gallery trajectories are confined to the tiny region $|\sin\chi| \gtrsim 0.99$.

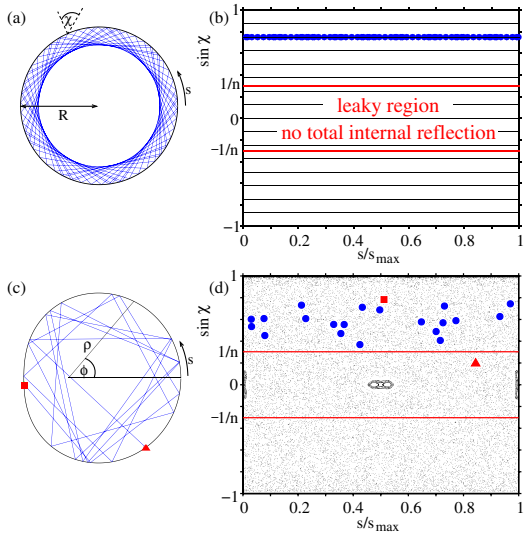

FIG. 1 (color online). (a) Whispering-gallery ray trajectory in the circular microdisk. (b) Poincaré SOS showing the trajectory (thick dots) in phase space; s is the arclength coordinate and χ is the angle of incidence. Typical trajectories fill a line of constant $\sin\chi$. The critical lines $\sin\chi_c = \pm 1/n$ enclose the leaky region. (c) Chaotic ray trajectory in the limaçon cavity with $\varepsilon = 0.43$. (d) Poincaré SOS for the trajectory (thick dots) starting above the critical line (square) and refractively escaping after only 20 bounces (triangle). The small dots show a typical trajectory in the corresponding closed billiard system.

While in the long-time limit the phase space of closed chaotic systems is essentially structureless, cf. Fig. 1(d), the phase space of an open chaotic system is structured by the so-called "chaotic repeller" [29]. It is the set of points in phase space that never visits the leaky region both in forward and backward time evolution. The stable (unstable) manifold of a chaotic repeller is the set of points that converges to the repeller in forward (backward) time evolution. The unstable manifold therefore describes the route of escape from the chaotic system. In the case of light, Fresnel's laws impose an additional, polarization dependent weighting factor to the unstable manifold in the leaky region [33], since at each reflection the intensity inside is multiplied by the Fresnel reflection coefficient.

Following Refs. [32,33] the unstable manifold can be uniquely computed as a survival probability distribution calculated from an ensemble of rays starting uniformly in phase space with identical intensity. Figure 2 depicts the resulting Fresnel weighted unstable manifolds for the limaçon cavity using 50 000 rays. Note the following: (i) In the leaky region, the manifold is concentrated on very few high-intensity spots. We therefore expect a highly directional FFP. (ii) While in the case of TE polarization one finds one spot with $\chi > 0$ (and another symmetry-related one at $s \to s_{\max} - s$, $\chi \to -\chi$), the TM polarization case possesses two of those.

The unstable manifold in the leaky region directly determines the FFP. Mapping the unstable manifold in Fig. 2 to the far field by using Snell's and Fresnel's laws (for generalization to curved interfaces, see [36,37]) we obtain Fig. 3. Note that the FFP is shown only for the upper half space (0°–180°); the lower half space is given by symmetry. For TE polarization, we find directionality around $\phi = 0$, whereas in the TM case additional, smaller peaks occur. The ray in the left upper inset represents one typical trajectory emitting to $\phi \approx 0$ (marked by arrows). The emitting bounce (marked 1, 1s is the symmetry-related counterpart), the three bounces before, and the one after (marked 2) are shown. Whereas the trajectories are equal for both polarizations, their intensities are different: As visible in the right inset, the rays escaping at 1 hit the line of the Brewster angle $|\chi_B| = \arctan 1/n < \arcsin 1/n$. In the TE case, transmission is nearly complete and no inten-

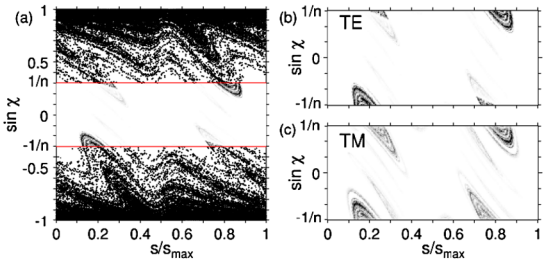

FIG. 2 (color online). (a) Fresnel weighted unstable manifold of the limaçon cavity for TE polarization. Magnification reveals the differences between TE (b) and TM (c) polarization in the leaky region, which originate from Fresnel's law.

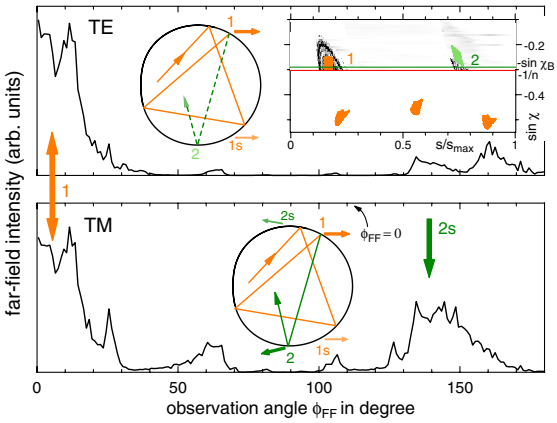

FIG. 3 (color online). Far-field emission pattern for TE (top) and TM polarization (bottom) calculated from an ensemble of rays on the unstable manifold in Figs. 2(b) and 2(c). The insets illustrate ray dynamics leading to directed emission. The dashed line has strongly reduced intensity due to reflection near the Brewster angle. Right inset: 250 rays were started in the rectangular region at 1 and followed forward (region at 2) and backward (the three regions below the critical line). $1s$ and $2s$ mark the symmetry-related bounces to 1 and 2.

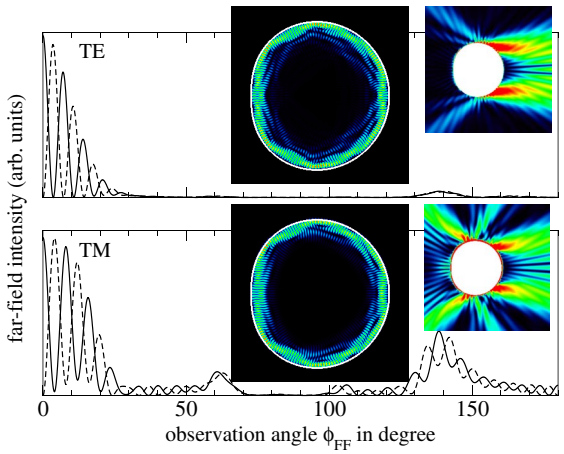

FIG. 4 (color online). Angular dependence of the electric far-field intensity for a TE mode of even (top, solid line) and odd parity (top, dashed) with $\Omega = 26.0933$, $Q \approx 185\,000$, and a TM mode of even (bottom, solid line) and odd parity (bottom, dashed line) with $\Omega = 25.8069$, $Q \approx 10^7$; cf. Fig. 3. The insets contain the near-field pattern of even-parity modes (middle) and its external structure (right).

sity can reach the next bounce 2. This causes the sharp decrease in the intensity that is more clearly visible in Fig. 2(b). The Fresnel law for TM polarization does not show the Brewster angle feature. Therefore, a significant percentage of the light is reflected toward bounce 2. Since bounce 2 emits into a different direction, an appreciable amount of intensity collects in a second far-field peak.

We have seen that chaotic ray dynamics can lead to highly directional emission. Does this result of geometric optics carry over to the wave optics? It has been demonstrated that the FFP of optical modes can be strongly influenced by the unstable manifold of the underlying ray dynamics [31–33]. A consequence is that for fixed polarization and cavity parameters the FFP is independent on the internal mode structure [34]. This raises the hope that the directionality observed in our ray simulations will survive in wave optics. To this end we solve Maxwell equations numerically using the boundary element method [38]. This approach gives the resonant frequencies ω, the intrinsic Q factors (measured Q factors will be reduced due to surface roughness and residual absorption [9]), and the spatial mode pattern. According to the discrete symmetry, even and odd modes are distinguished.

The top panel of Fig. 4 shows the near- and the far-field pattern of a high-Q TE mode. The normalized frequency $\Omega = \omega R/c = 26.0933$, c being the speed of light in vacuum, corresponds to, e.g., a free-space wavelength of about 900 nm for $R = 3.75\ \mu$m. Indeed, as predicted by our ray dynamical analysis the mode exhibits directional light emission around $\phi = 0$. The angular divergence of 24° is significantly smaller than the values reported for low-Q disks [23,24], and also less than in Ref. [27]. Moreover, for fixed polarization and cavity parameters, the FFPs of all high-Q TE modes in this cavity have a similar envelope even though the internal mode structure is in general different; see, e.g., the odd-parity mode (dashed line) in the upper panel which is quasidegenerate with the even-parity solution (solid line). For the high-Q TM modes the same is true with a slightly different FFP; see the lower panel of Fig. 4.

Whereas the ray and wave based FFPs in Figs. 3 and 4, respectively, agree remarkably well, other wave properties seem to contradict the ray simulations: (i) the modes do not look chaotic but spatially rather well confined; (ii) their Q factors reach the present limit achievable for semiconductor microdisks [9] and seem to be too large given the fast escape from the chaotic repeller.

To further investigate the character of these optical modes we consider the Husimi projection [39], representing the wave analog of the Poincaré SOS. From ray-wave correspondence one would expect that the Husimi projection is distributed uniformly over the unstable manifold. However, Fig. 5(a) demonstrates that the TE mode is localized around $|\sin\chi| \approx 0.86$ and has only exponentially small intensity in the leaky region which explains the high Q factor. A closer inspection [40] reveals that the mode intensity is enhanced around an unstable periodic ray trajectory [dots and inset in Fig. 5(a)] which is part of the chaotic repeller. This phenomenon is called scarring [30] and has been observed in several kinds of physical systems including microcavities [41–43]. Note that the other high-Q modes found in this system also exhibit localization along—in general other—unstable periodic rays. The Husimi projection of the TM mode in Fig. 4 looks similar (not shown). The localization is even stronger, leading to a higher Q factor.

Even though the Husimi projection has a small contribution in the leaky region, it is precisely this outgoing light

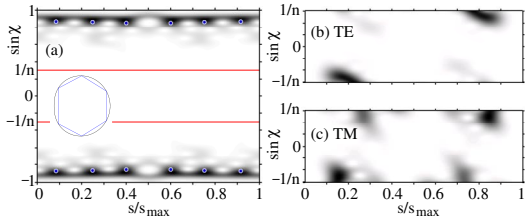

FIG. 5 (color online). (a) Husimi projection of the TE mode in Fig. 4; cf. Poincaré SOS in Fig. 1(d) and the unstable manifold in Fig. 2(a). The lines $\sin\chi_c = \pm 1/n$ enclosing the leaky region are indicated. The dots mark the periodic ray trajectory illustrated in the inset. Magnified Husimi projection in the leaky region for the TE (b) and TM (c) mode; cf. Figs. 2(b) and 2(c) for the ray simulation results.

that determines the FFP. Figures 5(b) and 5(c) show the Husimi projection in the leaky region. The convincing agreement with the unstable manifold in Figs. 2(b) and 2(c) demonstrates its responsibility for the directional emission, whereas scarring guarantees the high Q factor.

Note that, due to the observed agreement between ray and wave simulations, our results are also applicable to larger cavities. The particular deformation parameter $\varepsilon = 0.43$ is the optimum value for the localization of the discussed FFPs with $n = 3.3$ but highly localized FFP and high Q factors were also found for $0.41 \lesssim \varepsilon \lesssim 0.49$; i.e., fabrication tolerances are not crucial. Moreover, we tested that our results are robust against variations of the refractive index and remain valid for $2.7 \lesssim n \lesssim 3.9$.

In summary, we have proposed a deformed microdisk as a novel cavity design for robust directional light emission from high-Q modes. No complicated adjustment of geometry parameters is necessary, and the emission directionality is largely independent from wavelength, cavity size, refractive index, and the details of the interior mode structure. The latter finding is especially relevant for multimode lasing devices. We trace our, at first sight, counterintuitive results back to (i) wave localization along unstable periodic ray trajectories (scarring) ensuring high Q factors and (ii) escape of rays along the unstable manifold of the chaotic repeller ensuring directional emission. The simplicity of the cavity design allows for easy fabrication with a wide range of applications in photonics and optoelectronics. The discussed mechanisms are not restricted to disklike geometries but can, in principle, also be exploited for other geometries such as deformed microspheres and microtoroids.

We thank E. Bogomolny, H. Kantz, T.-Y. Kwon, J. Nagler, and M. Robnik for discussions. Financial support from the DFG research group No. 760 and the DFG Emmy Noether Programme is acknowledged.

[1] K. J. Vahala, Nature (London) **424**, 839 (2003).
[2] H.-G. Park *et al.*, Science **305**, 1444 (2004).
[3] S. M. Ulrich *et al.*, Phys. Rev. Lett. **98**, 043906 (2007).
[4] P. Michler *et al.*, Nature (London) **406**, 968 (2000).
[5] J. Reithmaier *et al.*, Nature (London) **432**, 197 (2004).
[6] E. Peter *et al.*, Phys. Rev. Lett. **95**, 067401 (2005).
[7] M. Schwab *et al.*, Phys. Rev. B **74**, 045323 (2006).
[8] S. L. McCall *et al.*, Appl. Phys. Lett. **60**, 289 (1992).
[9] C. P. Michael *et al.*, Appl. Phys. Lett. **90**, 051108 (2007).
[10] T. J. Kippenberg, J. Kalkman, A. Polman, and K. J. Vahala, Phys. Rev. A **74**, 051802(R) (2006).
[11] L. Collot *et al.*, Europhys. Lett. **23**, 327 (1993).
[12] M. L. Gorodetsky, A. D. Pryamikov, and V. S. Ilchenko, J. Opt. Soc. Am. B **17**, 1051 (2000).
[13] S. Götzinger *et al.*, Nano Lett. **6**, 1151 (2006).
[14] V. S. Ilchenko *et al.*, Opt. Lett. **26**, 256 (2001).
[15] D. K. Armani, T. J. Kippenberg, S. M. Spillane, and K. J. Vahala, Nature (London) **421**, 925 (2003).
[16] A. A. Savchenkov, V. S. Ilchenko, A. B. Matsko, and L. Maleki, Phys. Rev. A **70**, 051804(R) (2004).
[17] A. C. Tamboli *et al.*, Nat. Photon. **1**, 61 (2007).
[18] H. Lohmeyer *et al.*, Eur. Phys. J. B **48**, 291 (2005).
[19] A. F. J. Levi *et al.*, Appl. Phys. Lett. **62**, 561 (1993).
[20] J. U. Nöckel and A. D. Stone, Nature (London) **385**, 45 (1997).
[21] C. Gmachl *et al.*, Science **280**, 1556 (1998).
[22] T. Tanaka *et al.*, Phys. Rev. Lett. **98**, 033902 (2007).
[23] M. S. Kurdoglyan *et al.*, Opt. Lett. **29**, 2758 (2004).
[24] M. Kneissl *et al.*, Appl. Phys. Lett. **84**, 2485 (2004).
[25] J. U. Nöckel, A. D. Stone, and R. K. Chang, Opt. Lett. **19**, 1693 (1994).
[26] For a given total number of Bragg mirror pairs a micropillar can be optimized either with respect to the Q factor (roughly equal number of bottom and top mirror pairs) or directionality (otherwise).
[27] J. Wiersig and M. Hentschel, Phys. Rev. A **73**, 031802(R) (2006).
[28] H.-J. Stöckmann, *Quantum Chaos* (Cambridge University Press, Cambridge, 2000).
[29] A. J. Lichtenberg and M. A. Lieberman, *Regular and Chaotic Dynamics* (Springer, Berlin, 1992).
[30] E. J. Heller, Phys. Rev. Lett. **53**, 1515 (1984).
[31] H. G. L. Schwefel *et al.*, J. Opt. Soc. Am. B **21**, 923 (2004).
[32] S.-Y. Lee *et al.*, Phys. Rev. A **72**, 061801(R) (2005).
[33] S. Shinohara and T. Harayama, Phys. Rev. E **75**, 036216 (2007).
[34] S.-B. Lee *et al.*, Phys. Rev. A **75**, 011802(R) (2007).
[35] M. Robnik, J. Phys. A **16**, 3971 (1983).
[36] H. Schomerus and M. Hentschel, Phys. Rev. Lett. **96**, 243903 (2006).
[37] M. Hentschel and H. Schomerus, Phys. Rev. E **65**, 045603(R) (2002).
[38] J. Wiersig, J. Opt. A **5**, 53 (2003).
[39] M. Hentschel, H. Schomerus, and R. Schubert, Europhys. Lett. **62**, 636 (2003).
[40] R. Hegger, H. Kantz, and T. Schreiber, Chaos **9**, 413 (1999).
[41] S. B. Lee *et al.*, Phys. Rev. Lett. **88**, 033903 (2002).
[42] W. Fang, A. Yamilov, and H. Cao, Phys. Rev. A **72**, 023815 (2005).
[43] J. Wiersig, Phys. Rev. Lett. **97**, 253901 (2006).